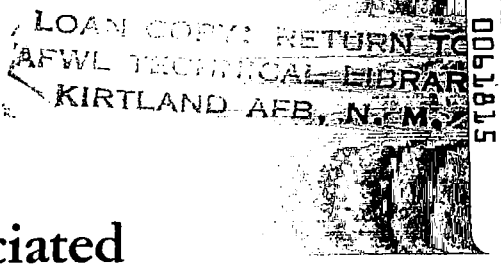

NASA Contractor Report 3158

Particle Dynamics Associated With the Spacelab Environment

V. A. Sandborn

CONTRACT NAS8-31688
JULY 1979

NASA

NASA Contractor Report 3158

Particle Dynamics Associated With the Spacelab Environment

V. A. Sandborn
Colorado State University
Fort Collins, Colorado

Prepared for
Marshall Space Flight Center
under Contract NAS8-31688

National Aeronautics
and Space Administration

Scientific and Technical
Information Branch

1979

Particle Dynamics Associated with the Spacelab Environment

by

V. A. Sandborn

SUMMARY

The problem of dust in the special environment of Spacelab is reviewed. A major factor of importance in the zero-gravity environment will be the presence of large particles. It is necessary to consider aerosol dynamics at Reynolds numbers larger than those of importance in the earth environment. The drag coefficient of particles in the range of Reynolds number from 1 to 100 is examined in detail. The accurate relation between the drag coefficient, c_D, and Reynolds number, R_e, for the range $1<R_e<100$ was found to be

$$c_D = \frac{24}{R_e}\left[1 + \frac{R_e^{0.7}}{6.8}\right]$$

Based on drag data for spheres currently available for slip and free molecular flow a general graphic correlation for the drag coefficient as a function of Reynolds and Knudsen number was developed.

The general equations that govern the dust dynamics were reviewed.

INTRODUCTION

Particle dynamics associated with the special environment of Spacelab may pose a new set of problems. The near zero value of gravitational forces will greatly reduce sedimentation of both large and small particles. The problem is further augmented by the presence of "g-jitter" effects associated with the space craft. Large particles, which would be created in an industrial use of the zero-g environment, could pose a major difficulty. Under the influence of gravity the large "dust" particles created, in for example a machining process, quickly settle out and do not pose a problem. In the Spacelab environment the large particles would float free and would also detach from solid surfaces easily. The slight variation in gravity (g-jitter) associated with Spacelab would act to keep the large particles in suspension.

A great deal of information, both experimental and theoretical has been obtained on the dynamics of fluid-solid suspensions, ref. 1 through 5. Attention has been focused heavily on the dynamics of small aerosol particles, since the newly developed laser velocimeters employ aerosols as tracers to measure fluid motion. Problems associated with aerosol particle motion in turbulent fluid flows were considered in detail by Lumley, ref. 6. In general the small aerosol particles can follow approximately the local turbulent motion, so that detailed information on the turbulent motion is obtained with the laser systems. The small particles would not pose a major problem in Spacelab, as they could be trapped on filters in a common air cleaning process. The large particles, because of their inertia, will not respond as quickly to the local fluid motion. Thus, it may not be possible to filter out the large particles as efficiently as the small particles in the Spacelab atmosphere. Either a larger air flushing system in Spacelab, or limitation on dust generation, may be required.

GENERAL IDENTIFICATION OF AEROSOL PARTICLES

Particles of interest in the spacelab environment will most likely be generated by the disintegration of solids. There is also the possibility of gas-to-particle generation in industrial application. Liquid particles might also be generated in certain experiments. Each of these types of particles will be referred to as aerosols. The aerosols will be assumed to be inert with respect to the spacelab atmosphere. In general, Hidy and Brock, ref. 3, have pointed out that the first criterion for defining an "aerocolloidal system" involves a "small" rate of settling of the suspended particles. Thus, the present discussion will fall in the broad spectrum of aerocolloidal systems.

Particle Size - The jargon employed in aerosol science refers to; dust as solid particles produced bydisintegration, smoke or fumes as particles formed from gases, and mist as liquid droplets. A very wide range of sizes and masses exist for aerosols. Friedlander, ref. 5, estimates that aerosol sizes can vary by factors of 10^5, while the mass can vary by factors of 10^{15}. For the special environment of spacelab the range of sizes and masses may be even greater. The minimum size of an aerosol will be that of a "molecular cluster", which is of the order of 10Å. Obviously, the very small molecular clusters are not likely to be as important in the present discussion as the larger dust particles. Particles formed directly from the gas state are usually less than a micron in size (1 micron = 10^{-6} meters, and is usually written as $1\mu m$). Dust particles range from $0.1\mu m$ up to $100\mu m$ for atmospheric type cases. Again the large "dust" particles generated in machining processes are greater than $1000\mu m$ in size.

If the particle is spherical in shape it is obvious that the size or characteristic length will be the diameter. If the particle is not spherical then the characteristic length will be related to a aerodynamic dimension. The aerodynamic dimension, or equivalent

"effective" diameter would be defined based on the drag of the particle. The effective aerodynamic diameter is determined by use of a cascade impactor. The cascade impactor is one instrument commonly used to classify aerosol sizes. The instrument consists of a series of collector plates, as shown on figure 1. Both

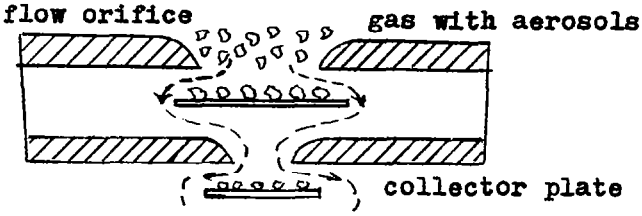

Figure 1. Cascade impactor.

the sizes of the orifices and the clearance between the orifice and the collector plates are varied from one stage to the next. The gas flow velocity is progressively increased for each stage so that smaller and smaller particles fail to turn with the flow and are collected on the plates. Any number of stages may be employed to obtain a measure of the size distribution of aerosols. The efficiency of a stage is a function of the Stokes number

$$S_t = \frac{c_s \rho_p U d_p^2}{18 \mu d} \qquad (1)$$

where

c_s slip correction factor
ρ_p particle density
U gas velocity through the orifice
d_p is the effective particle diameter
μ is the gas viscosity
d is the orifice diameter

Thus, the effective aerodynamic diameter can be defined as the diameter of a hypothetical sphere of unit density with the same Stokes number as the particle in question. The efficiency of the stages of a cascade impactor is such that a range of particles will be caught. Thus, in practice the stage is usually identified by a Stokes number which corresponds to the 50% impation efficiency level.

Cadle, ref. 7, describes a number of different methods that have been developed to define particle sizes. One technique that is the "equivalent" circle whose area is equal to the projected area of the particle. Special graticules have been developed to allow the particles to be evaluated under a microscope. For the present discussion it would appear that the aerodynamic specifications of particle characteristic size will be the logical parameter.

The aerosols of interest will be polydispersed in size with a range far greater than that encountered in a gravitional environment. The physical description of importance will be the size distribution function. For a given position in space the number of particles per unit volume can be determined if the size distribution function, n, is known. The number of particles, N, with sizes in the volume range V to $V+dV$ is

$$\Delta N = ndv \qquad (2)$$

For near spherical particles the distribution function might better be expressed in terms of the effective diameter, d_p rather than the volume. The relation between the volume and diameter distribution function, n_d, is, (Friedlander, ref.5)

$$n_d = \frac{\pi d_p^2 n}{2} \qquad (3)$$

Development of the time history of the particle distribution function within spacelab will be necessary to define the specific dust problems.

Four specific effects can be identified in the time history of the distribution function:

1. Nucleation - formation of particles from the gas phase.
2. Coagulation - clumping of particles.
3. Sedimentation - fall out of particles due to gravitational forces.
4. Diffusion - Browian motion and flow convection produces diffusion of the particles.

Nucleation and coagulation are processes which occur within the volume, dv, of gas, while sedimentation and diffusion represent transport across the volume boundaries. For the application to spacelab, sedimentation must be viewed as a highly time dependent phenomenon, due to the "g-jitter" aspect of the craft. Within the global aspects of the spacelab problem, the "sticking" of particles to the surfaces must also be considered. While small particles may adhere to surfaces they come in contact with, the large particles will easily pull away when changes in acceleration occur.

Friedlander, ref. 5, suggests the distribution function be divided as follows

$$\frac{dn}{dt} = \left[\frac{dn}{dt}\right]_i + \left[\frac{dn}{dt}\right]_e \tag{4}$$

where i corresponds to the processes internal to the volume and e corresponds to the processes external to the volume. The moments of the distribution function

$$M_n = \int n_d d_p^N d(d_p) \tag{5}$$

can be related to specific physical properties:

1. M_0 gives the total concentration of particles in suspension at a given location.
2. M_1 divided by M_0 is the average diameter, $\bar{d}_p$, of the particles in suspension.
3. M_2 times π gives the total surface area per unit volume of particles, and the average surface area is given by $\pi M_{2/M_0} = \bar{A}$.
4. M_3 times $\pi/6$ gives the total volume of the particles, and the average volume is obtained by dividing by M_0.
5. M_4 is proportional to the total surface area of the particles that sediment from the volume of fluid.
6. M_5 is proportional to the mass flux of particle sedimentation from the fluid.
7. M_6 is proportional to the scattering of light from particles that are smaller than the wave length of the incident light.

Obviously the larger particles will contribute greater, or dominate the higher moments of the distribution function.

The possible shapes of the size distributions are reviewed by Cadle, ref. 7. A common occurring probability function for dust particles in nature is the log-normal distribution. The log-normal distribution is skewed, in that the probability of finding very small particles drops off rapidly, while the probability of large particles occurring is more likely. The skewed distribution is expected to occur in spacelab since the lack of sedimentation will act to increase the number of large particles in suspension. Also the very small particles will be more likely to stick to exposed surfaces and thus diffuse out of the atmosphere of spacelab.

DEVELOPMENT OF THE EQUATIONS GOVERNING DUST DYNAMICS

A general relation for the time rate of change of the size distribution function, n, can be developed from equation (4). Formulation, coagulation and growth are processes internal to a given volume, while diffusion and sedimentation involve transports across the walls of the volume.

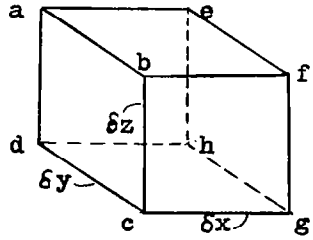

Figure 2. Elemental Volume.

External Processes - For the volume a, b, c, d, e, f, g, h, shown in figure 2 the net accumulation of particles within the element due to convection is

$$\text{Convective Accumulation} = -\delta x \delta y \delta z \left[\frac{\partial nu}{\partial x} + \frac{\partial nv}{\partial y} + \frac{\partial nw}{\partial z}\right] \qquad (6)$$

where u, v, and w are the components of the convective velocity vector V. The accumulation of particles due to diffusion is

$$\text{Diffusion Accumulation} = \delta x \delta y \delta z D \left[\frac{\partial^2 n}{\partial x^2} + \frac{\partial^2 n}{\partial y^2} + \frac{\partial^2 n}{\partial z^2}\right] \qquad (7)$$

where D is the diffusion coefficient. Equation (7) is for an

isotropic fluid with equal diffusion in all three directions.

Sedimentation is related to an external gravitational force field, which will be very small and varable for the spacelab environment. Other force fields, either electrical or thermal, may also be present in spacelab of equal strength to that of gravity. If a force field is present the particles will migrate in the direction of the force with a velocity, c, given by

$$c = \frac{F}{f} \tag{8}$$

where F is the force and f is the resistance to motion of the particles due to fluid drag or friction. The accumulation of particles due to a force field can be written as

$$\text{Force Field Accumulation} = \delta x \delta y \delta z (c_x n + c_y n + c_z n) \tag{9}$$

The rate of particle accumulation in the volume $\delta x\, \delta y\, \delta z$ due to convection, diffusion and external force fields can be written as

$$\left(\frac{\partial n}{\partial t}\right)_e = -\vec{v} \cdot \nabla n + D\nabla^2 N - \nabla \cdot \vec{c} n \tag{10}$$

In this equation the velocity, $\vec{v}$, is for the most part independent of the particle concentration, and dependent on the fluid mechanics of the system considered. For spacelab application the velocity would be due to the air exchange system within the working area. Obviously, if large particles must be drawn into the air cleaning filters, then the magnitude of $\vec{v}$ will be large. The flow within the working area will be complex and not easily predicted, due to the obstructions and personnel.

The diffusion coefficient, D, and the drift velocity, $\vec{c}$, will both depend on the particle size. The diffusion coefficient decreases as the particles become large. For a constant force field, which is independent of particle size, the drift velocity

will decrease as the particles become larger. The friction factor, f, in equation (8) is directly proportional to the particle diameter for the small particles. In the "Stokes" flow region the friction factor for a sphere is

$$f = \frac{3\pi\mu d_p}{C_s} \tag{10}$$

where μ is the fluid coefficient of viscosity, d_p is the particle diameter and C_s is a slip correction factor. For large particles above the Stokes flow regine, the friction factor may be less dependent on diameter than that given by the Stokes relation.

Obviously there are many cases when the force field will also be a function of the particle size. Gravitational forces will increase as the mass of the particle. Thus, it is difficult to specify how the drift velocity will vary with particle size.

Internal Process - The internal processes of growth and coagulation of particles have been treated in detail by Friedlander, ref. 5. For growth the net rate of change in particle number in the elemental volume $\delta v = \delta x \delta y \delta z$ is, ref. 5,

$$\left(\frac{\partial n}{\partial t}\right)_g = -\frac{\partial I}{\partial v} \tag{11}$$

Which is a particle continuity relation. $I(v,t)$ is the particle flow "current" or the number of particles per unit time per unit volume of gas passing a point δv .

When particles collide some will adhere together resulting in larger particles. Coagulation produces large particles from the smaller particles, which results in the skewed log normal type of particle distributions. Friedlander, ref. 5, gives the following formulation for the coagulation

$$\left(\frac{\partial n}{\partial t}\right)_{coag} = \text{Formation} - \text{Loss} \tag{12}$$

When any two particles of volumes v_1, and v_2 adhere to form a new particle the number density of particles is reduced by one.

Obviously, the formation rate will depend directly on how often particles collide. Employing a "collision frequency function", $\beta(V_1, V_2)$ such that the collision rate can be expressed as

$$\text{Collision Rate} = \beta(V_1, V_2)\, n(V_1)\, n(V_2)\, dV_1\, dV_2$$

Thus the formation of particle of size V_1, from the collision of smaller particles of size $(V_1 - V_2)$ and V_2 is

$$\text{Formation over } dV_1 = \frac{1}{2}\int_0^{V_1} \beta(V_2, V_1 - V_2)\, n(V_2)\, n(V_1 - V_2)\, dV_2\, dV_1$$

and the loss of particles of size V_1, due to collisions with other particles is

$$\text{Loss Over } dV_1 = \int_0^{\infty} \beta(V_1, V_2)\, n(V_1)\, n(V_2)\, dV_1\, dV_2$$

The net rate of formation of particles given by equation (12) is

$$\left(\frac{\partial n}{\partial t}\right)_{COAG} = \frac{1}{2}\int_0^{V_1} \beta(V_2, V_1 - V_2)\, n(V_2)\, n(V_1 - V_2)\, dV_2 - \int_0^{\infty} \beta(V_1, V_2)\, n(V_2)\, n(V_1)\, dV_2 \qquad (13)$$

Dynamic Equation = The general dynamic equation for the size distribution function is

$$\frac{\partial n}{\partial t} + \nabla \cdot n\vec{V} + \frac{\partial I}{\partial V} = \nabla \cdot D\nabla n + \frac{1}{2}\int_0^{V_1} \beta(V_2, V_1 - V_2)\, n(V_2)\, n(V_1 - V_2)\, dV_2 - \int \beta(V_1, V_2)\, n(V_1)\, n(V_2)\, dV_2 - \nabla \cdot \vec{c}\, n \qquad (14)$$

For the case of incompressible flow, which would be the flow encountered on the space laboratory filtering system

$$\nabla \cdot n\vec{V} = \vec{V} \cdot \nabla n \qquad (15)$$

AEROSOL DRAG FORCES

Removal of dust from an environment depends mainly on the movement of air through a filter system. For the specific spacelab environment filters will be of major importance, as gravitational sedimentation will not be present. Thus, the drag forces on the aerosols will be the basic mechanism for the management of dust in the spacelab. The general view of external processes considered in the previous section employed a friction factor, f,

to represent the drag force on the particles. It was also noted that the size distribution of particles can be expressed in terms of a Stokes number, eq. (1), which was directly related to the particle aerodynamic drag. In this section a review of the drag process is covered, and the areas of specific interest to spacelab are identified.

The size and shape of dust particles that will be present in the spacelab environment can not be specified. As noted earlier, it is obvious that much larger sized particles can be expected due to the absence of sedimentation. It is also possible that some reduction in the number of very small particles will occur due to their attachment to the very large particles not normally present in gravitational force fields. Although the aerosols found in spacelab are not expected to have a well defined shape, the present discussion will consider first the ideal spherical particle. As noted in the discussion on size distributions it will be convenient to describe random shaped particles in terms of an equivalent "aerodynamic" spherical diameter.

Sphere Drag - For the discussion of drag it is convenient to employ a non-dimensional drag coefficient C_D defined as

$$C_D = \frac{F}{(\pi r^2)\frac{1}{2}\rho U^2} \qquad (16)$$

where $F(\equiv cf)$ is the force on the sphere, as employed in equation (8), ρ is the air density, U is the air velocity, and πr^2 is the frontal area of the sphere. The drag coefficient is found to be a function of the non-dimensional parameters, Reynolds number, Knudsen number and in the general case the Mach number also. The Reynolds number expresses the ratio of the inertia force to the viscous force of the flow. For the spacelab application the Reynolds number will be the main factor in the determination of the drag on the aerosol particles. The Knudsen

number is the ratio of the mean free path between molecules of air to the sphere diameter. For large Knudsen number the drag approaches the free molecular flow value, while small Knudsen number flows produce continuum flow results. Aerosol problems normally are found to contain many particles in the region between continuous and free molecular flow. For spacelab considerations the possibility of a great number of large particles may make Knudsen number considerations of only limited interest. The Mach number is the ratio of the flow velocity to the speed of sound. Mach number effects are limited to high velocity flows in the continuum regine. Mach number effects are not important in the spacelab dust management considerations.

Figure 3 shows the values of both Knudsen and Reynolds number as a function of sphere diameter. The environment of spacelab will be nearly that of a standard atmosphere, with a mean free path of 0.065 microns. Reduction of the pressure or more likely an increase in temperature will produce slight increases in the mean path. The curve labled 1/2 atmosphere represents an upper limit on the variation of Knudsen number that might be expected in the spacelab environment. Knudsen numbers of the order of 5 to 10 are required for free molecular flow. In the range of Knudsen numbers between 5 and 10^{-3} the flow is referred to as "slip flow", since the flow velocity is not zero at the sphere surface. For Knudsen number less than roughly 10^{-3} the flow can be treated as a continuum, and no slip occurs at the sphere surface.

The Reynolds number determines whether the flow around the sphere is dominated by the viscous forces or the inertia forces. For Reynolds numbers less than roughly 0.1, inertia forces can be neglected completely. The classical Stokes solution for the drag of spheres, eq. (10), is for the case where inertia terms are neglected. The Stokes solution in terms of the drag coefficient and the Reynolds number may be written as

$$c_D = \frac{24}{Re} \qquad (17)$$

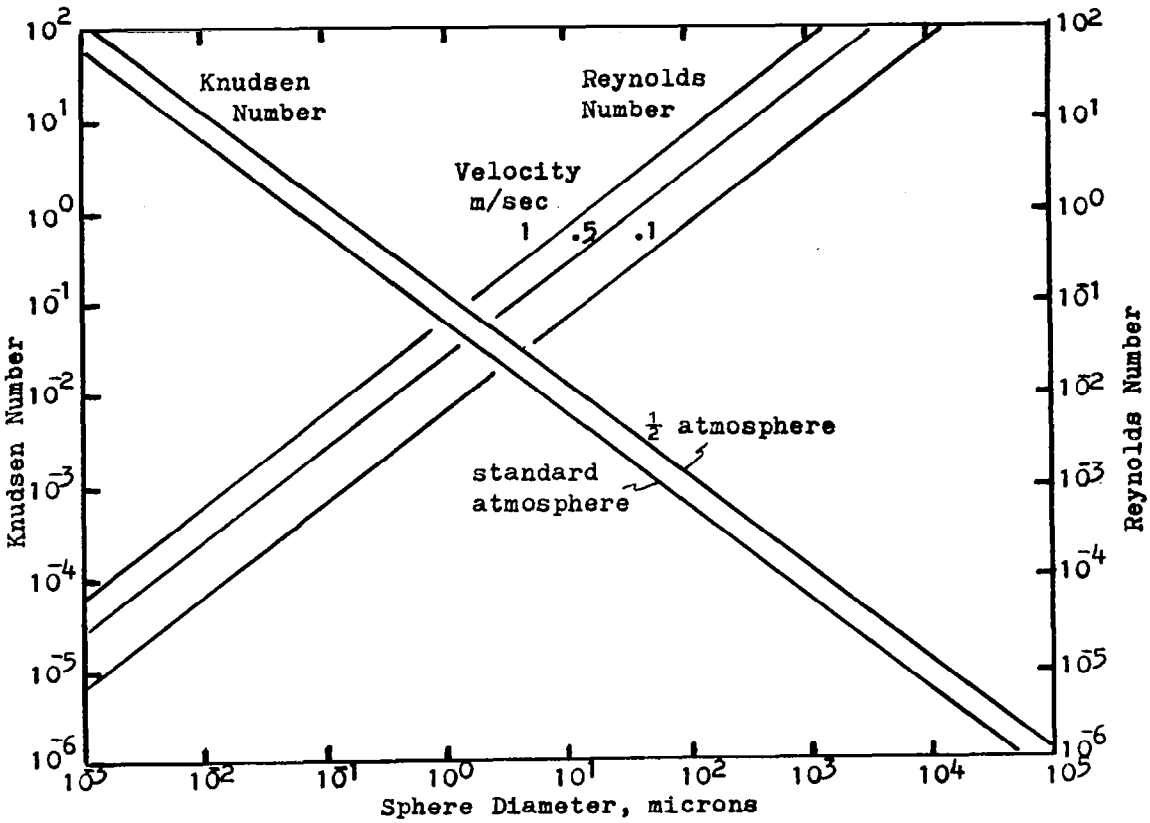

Figure 3. Variation of Knudsen and Reynolds numbers with sphere diameter.

For Reynolds numbers below 0.1 the relation is very close to the actual measured drag coefficients. The relation is roughly 10% too low for a Reynolds number of 1. Oseen, ref. 8, employed a simplified model for inertia to obtain a second order approximation to the sphere drag at low Reynolds numbers

$$c_D = \frac{24}{Re}\left(1 + \frac{3Re}{16}\right) \qquad (18)$$

This solution improves the prediction of drag up to a Reynolds number of roughly 0.5. It over predicts the drag by 7% at a Reynolds number of 1. Further development of the Oseen approach lead to the inclusion of higher order Reynolds number terms, however the improvement over the predictions of equation (18) is very minor. At Reynolds numbers greater than 1 the viscous boundary layer

developed on the sphere starts to alter the flow around the particle. Above a Reynolds number of approximately 40, separation of flow from the rear surface of the sphere becomes pronounced. At much higher Reynolds numbers, outside the area of interest for aerosol problems, the viscous constraints become small compared to the inertia terms and turbulent flow developes. In the area of interest to the spacelab problem, the Reynolds numbers are not expected to be greater than 100.

For the drag of spheres in the range of $1<R_e<400$ the empirical relation proposed by Klyachko, ref. 9, is found to fit the experimental results within 2%

$$C_D = \frac{24}{Re}\left(1 + \frac{Re^{2/3}}{8}\right) \qquad (19)$$

For the spacelab study it might appear that the interest will be for Reynolds numbers less than 100, fig. 3. A comparison of equation (19) with measured values of C_D (compiled by Fucks, ref. 2) is shown in figure 4. In the Reynolds number range from approximately 3 to 100, equation (19) is slightly low. A somewhat improved fit to the experimental can be obtained by adjusting the constant of equation (19) to

$$C_D = \frac{24}{Re}\left(1 + \frac{Re^{0.7}}{6.8}\right) \qquad (20)$$

Equation (20) is also plotted on figure 4. Equation (20) gives a slightly more accurate comparison with the data in the range of interest for spacelab conditions.

As noted previously the drag depends not only on the Reynolds number, but also on the Knudsen number. The data of figure 4 is for the continuum flow conditions where the Knudsen number is very small. As noted in equation (10), if the Knudsen number is of the order of 10^{-1} or greater it is necessary to employ a slip flow correction for the drag coefficient. At this point it is not obvious that the small particles, which correspond to the

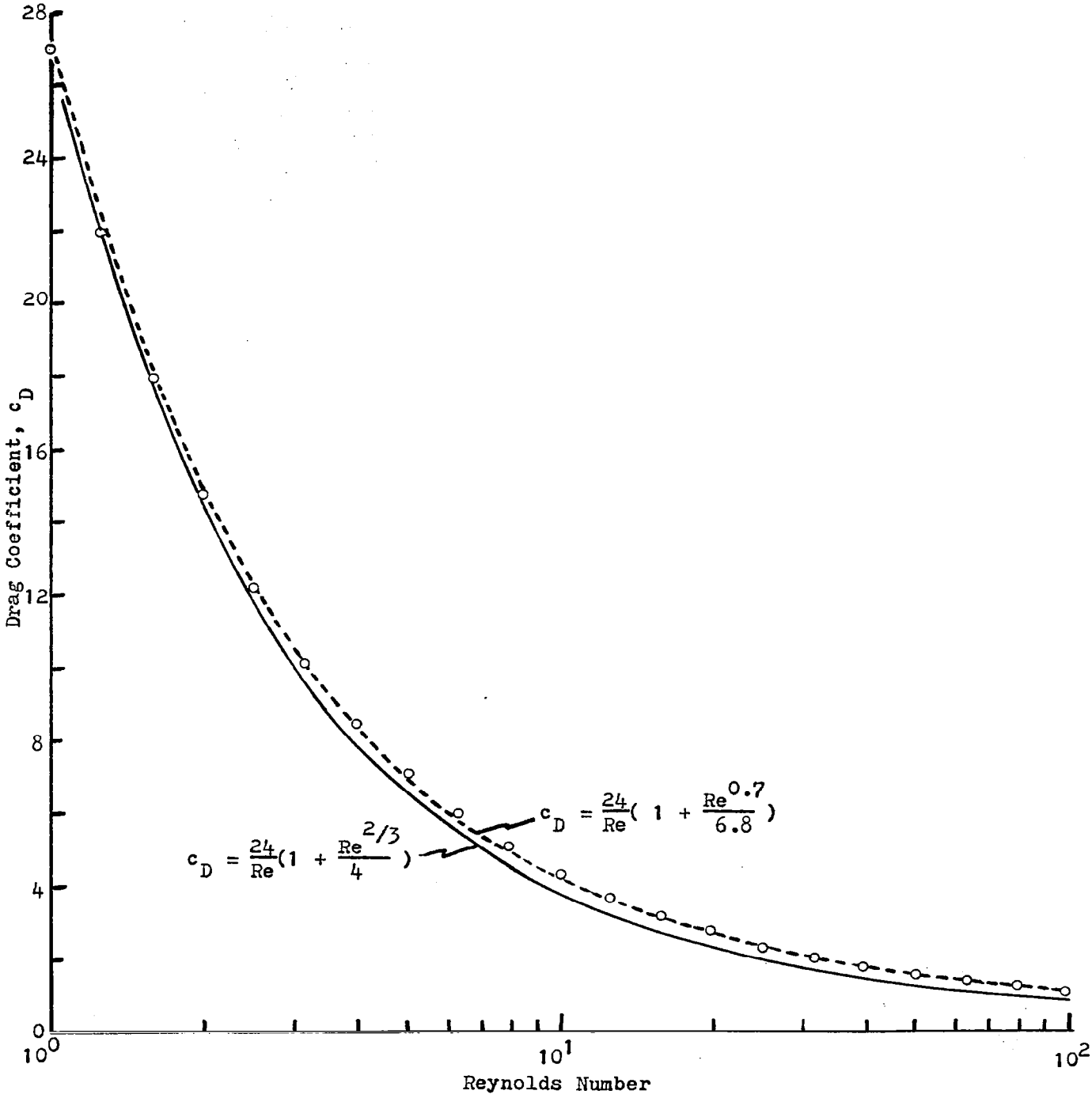

Figure 4. Curve fit of the sphere drag coefficient at moderate Reynolds numbers.

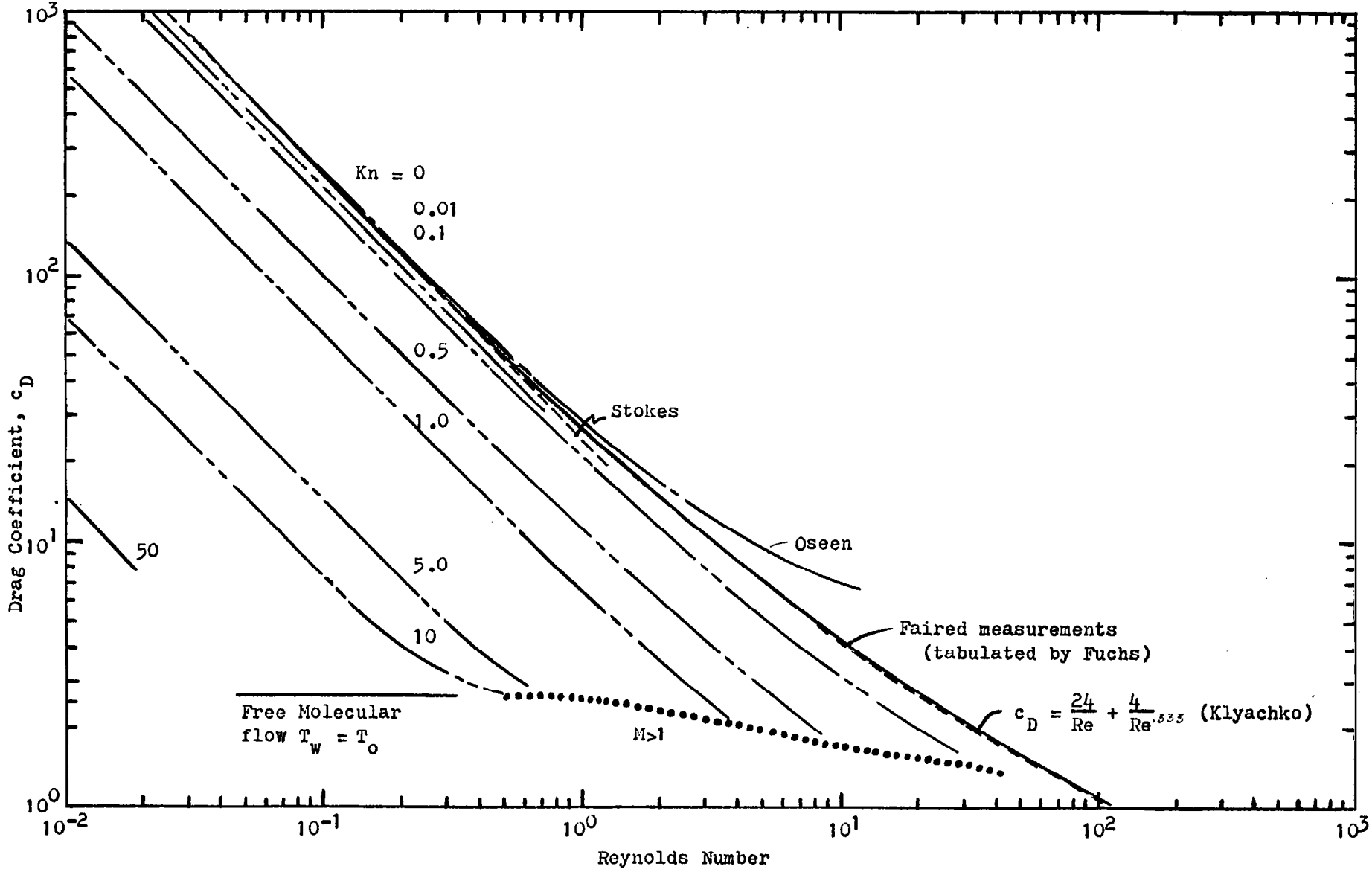

Figure 5. General drag coefficient correlation for spheres.

larger Knudsen numbers, will be of major importance in spacelab conditions.

The "slip" flow correction for the drag of a sphere, C_S, was developed by Millikan, ref. 10,

$$C_S = 1 + 2\,Kn\,(A + B\,e^{-\frac{C}{2Kn}}) \qquad (21)$$

where A = 1.257, B = 0.400 and C = 0.55, ref. 11.
Figure 5 was developed, using equation (19) divided by equation (21), to determine the different Knudsen number curves. For the spacelab application the slip flow conditions are probably limited to Reynolds numbers less than 10^{-1}. However, to define the expected extent of the complete sphere drag map the limiting case of large Mach number drag measurements, ref. 12 and 13, is also plotted on figure 5. For large Mach numbers (or more important to free molecular flow, large speed ratios) a limiting value of C_D is applicable for Knudsen numbers greater than 5 to 10. For smaller Knudsen numbers it is not possible to theoretically predict the limiting value of C_D. Experience with heat transfer measurements for spheres, ref. 14, and cylinders, ref. 15, suggest that the results for Mach numbers greater than roughly 2 gives a limiting lower value for C_D. No doubt the Knudsen number curves may fair more smoothly into the high Mach number measurement, although the region of intersection between the curves drawn are at the correctly measured Knudsen number.

Also shown on figure 5 are the Stokes, eq. (17), and Oseen, eq. (18), relations for the low Reynolds number continuum flow. As pointed out by Fucks, ref. 2, the Oseen correction to the Stokes relation is only usable in a very limited Reynolds number range. The emprical relation of Klyachko, ref. 9, or the relation given as equation (20) can better approximate the drag at "high" Reynolds number than either the Stokes or Oseen relations.

The free molecular flow limit shown on figure 5 corresponds to the upper limit of speed ratios obtained from theoretical considerations, ref. 16. This limit will not be encountered in the environment of space lab.

Non-Spherical Particles. - The spherical particle is at best a highly idealized model of the aerosols that will be encountered in the spacelab environment. It is not possible to develope a drag "map" for each shape of particle encountered. Only the sphere and ellipsoids have been evaluated in detail. The ellipsoid can include the limiting shapes of a cylinder and at the other limit a thin elliptical plate or disk. Studies of ellipsoidal particles have received considerable attention, ref. 2.

Somewhat surprising it is found that the elliptical particle in a gravitational field will not have a preferred direction of orientation in a low velocity, uniform, viscous flow. This result, that the torque acting on an ellipsoid of revolution will be zero, has been observed both experimentally and analytically. Obviously particles which are not symetric in shape will develope torques which will result in a preferred direction of orientation. In a gravitational free fall, elongated particles orient themselves in a way that balances the troque due to drag with the gravitational force. As a result, the orientation that produces either a minumum drag or torque may not be the preferred orientation in a gravitational free fall. In the absence of gravity, as encountered on spacelab, the orientation will depend more heavily on the torque developed by the drag forces. The g-jitter encountered in the gravitational field of spacelab will produce a random force on the particles, which could cause an oscillation in the orientation. In the absence of a constant gravitational force erratic motion, such as spiral, zigzag or gliding trajectories of the aerosol particles would not be encountered.

The theoretical evaluation of the drag of ellipsoids for the purely viscous flow regine results in a solution similar to the Stoke's solution for a sphere, eq. (10). Only the numerical coefficient is changed to account for the change in shape, ref. 17. A numerical coefficient, D_s, which is a function of the shape of the particular spheroid, is used to correct the Stokes value.

For a prolate ellipsoid (rotation of an ellipse about its major axis) with motion along the polar axis, the shape coefficient is

$$D_s = \frac{\frac{4}{3}\left[\left(\frac{a}{b}\right)^2 - 1\right]}{\frac{2(a/b)^2-1}{((a/b)^2-1)^{\frac{1}{2}}} \ln\left[(a/b)+\sqrt{(a/b)^2-1}\right] - (a/b)} \qquad (22)$$

where a/b is the ratio of the major to the minor axis of the ellipsoid. For the probate ellipsoid with motion transverse to the polar axis the shape coefficient is

$$D_s = \frac{\frac{8}{3}\left[\left(\frac{a}{b}\right)^2 - 1\right]}{\frac{2(a/b)^2-3}{[(a/b)^2-1]^{\frac{1}{2}}} \ln\left[(a/b)+\sqrt{(a/b)^2-1}\right] + (a/b)} \qquad (23)$$

For an oblate ellipsoid (rotation of an ellipse about its minor axis) with motion along the polar axis the shape coefficient is

$$D_s = \frac{\frac{4}{3}\left[\left(\frac{a}{b}\right)^2 - 1\right]}{\frac{(a/b)[(a/b)^2-2]}{[(a/b)^2-1]^{\frac{1}{2}}} \text{ARCTAN}\left[(a/b)^2-1\right]^{\frac{1}{2}} + \left(\frac{a}{b}\right)} \qquad (24)$$

For the oblate effipsoid with motion transverse to the polar axis the shape coefficient is

$$D_s = \frac{\frac{8}{3}\left[\left(\frac{a}{b}\right)^2 - 1\right]}{\frac{(a/b)[3(a/b)^2-2]}{[(a/b)^2-1]^{1/2}} \text{ARCTAN}\left[(a/b)^2-1\right]^{\frac{1}{2}} - \frac{a}{b}} \qquad (25)$$

Figure 6 is a plot of the drag coefficient for a number of the possible ellipsoid shapes computed from equations (22) through (25). The equatorial axis of the ellipsoid is the characteristic used to define the Reynolds number. The oblate ellipsoid produces drags less than the sphere, while the prolate ellipsoid produces a drag approaching that of a disk.

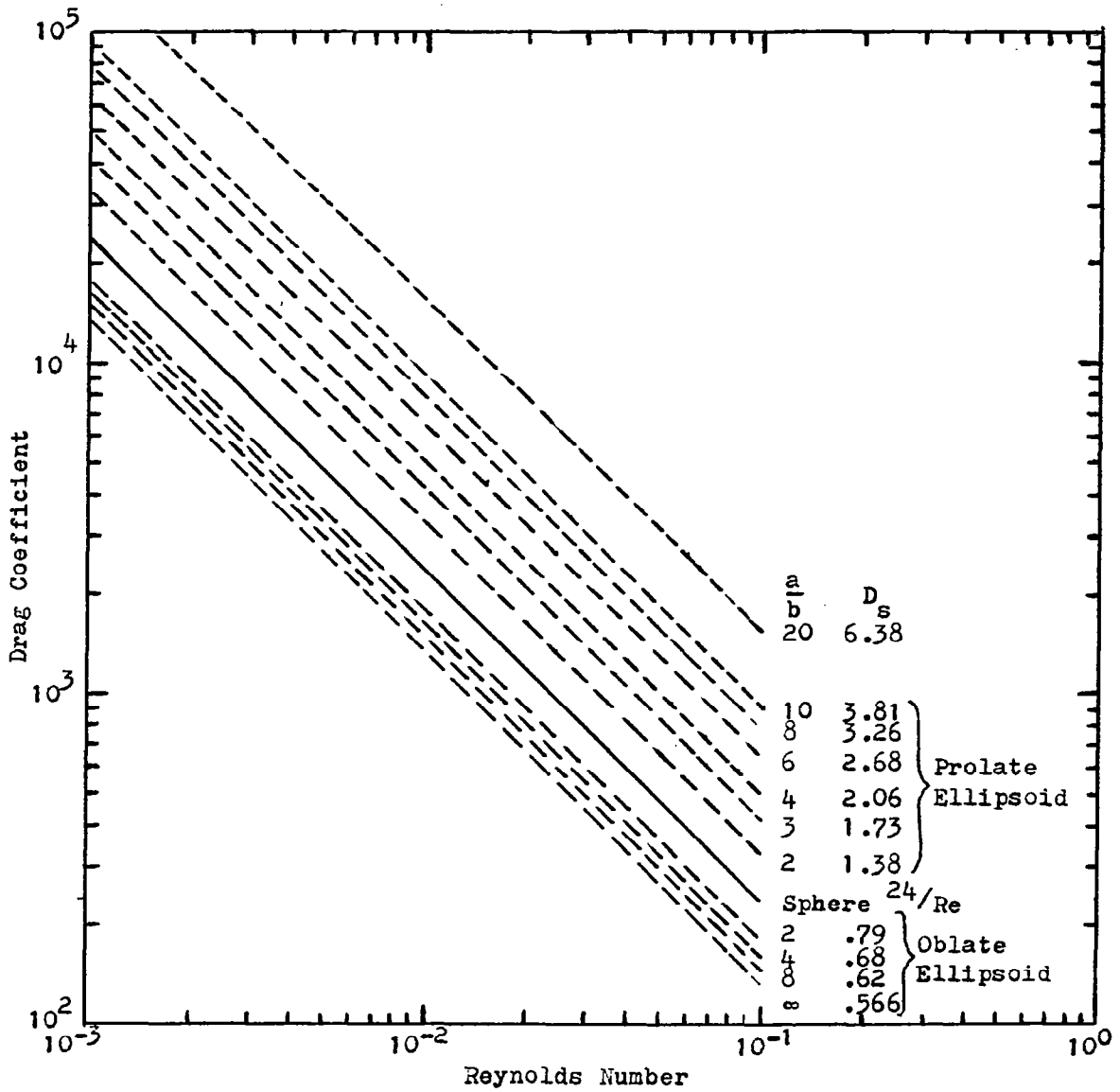

b) Flow transverse to the polar axis.

Figure 6. (Concluded) Drag coefficient of ellipsoid shapes.

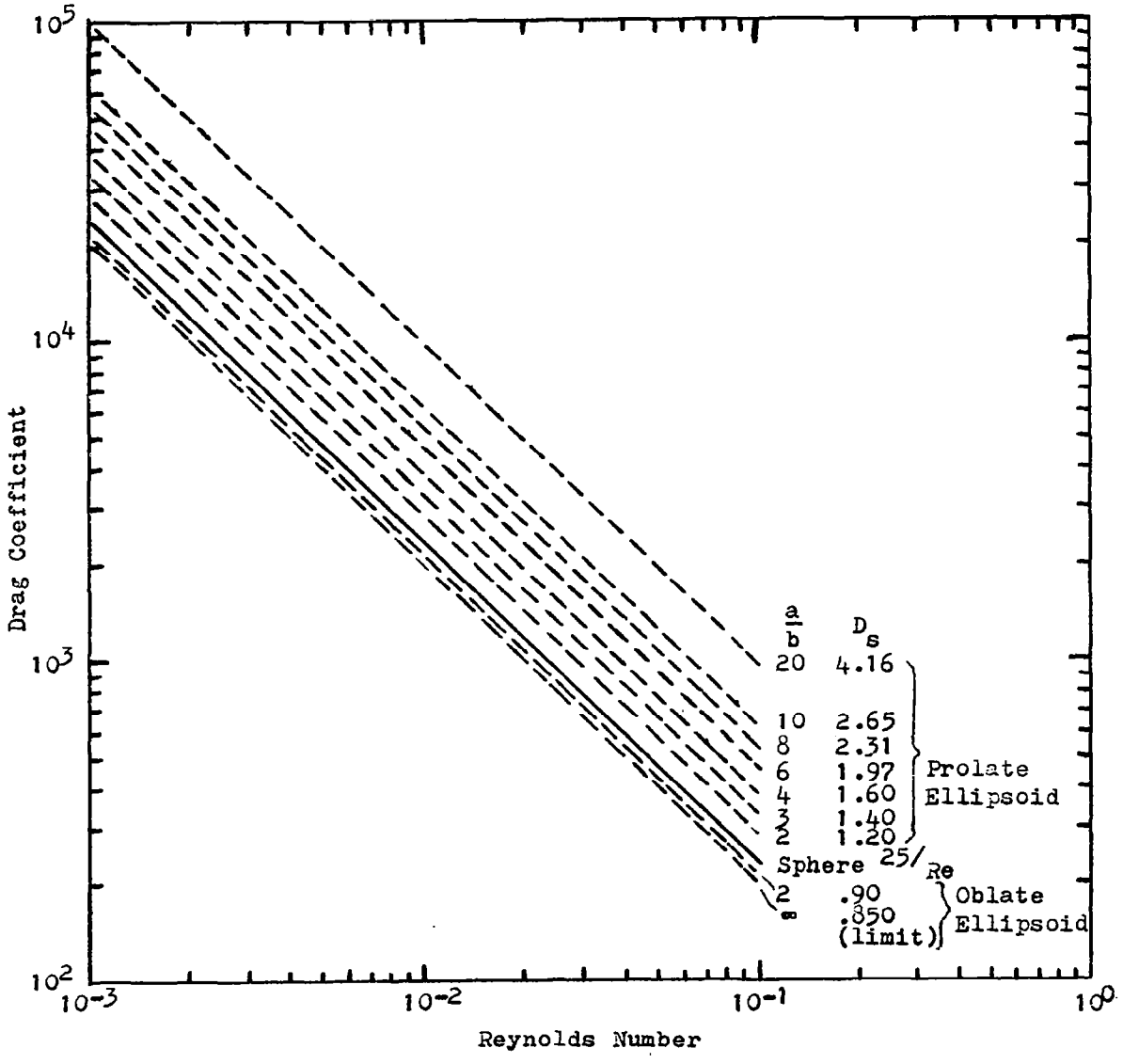

a) Flow along the polar axis.

Figure 6. Drag coefficient of ellipsoid shapes.

For orientation of the ellipsoid at angles rather than parallel or transverse to the polar axis the drag can be resolved into components. If the particle is rotating (due to Brownian motion) it can be shown that the average resistance is equivalent to the polar axis being oriented parallel to the flow one-third of the time and perpendicular to the flow two-thirds of the time, ref. 2. A statistical mean resistance can be computed using the 1/3 and 2/3 rule.

In the discussion of particle size it was noted that an effective diameter, d_e, could be defined such that the drag of the particle corresponds to that of an equivalent sphere. For the ellipsoids the equivalent diameter is $d_e \left(\frac{a}{b}\right)^{1/3}$ for the prolate and $d_e \left(\frac{a}{b}\right)^{-1/3}$ for the oblate case, where d_e is the equatorial diameter, Fucks, ref. 2, suggests the use of a "dynamic" shape factor, which is the square of the ratio of the equivalent diameter of the particle to that of a sphere of the same volume. The dynamic shape factor is similar to the use of a Stokes number, eq. (1), to define particle characteristics. Listed below are typical dynamic shape factors for a number of characteristic particles.

TABLE 1. TYPICAL DYNAMIC SHAPE FACTORS
(FOR A RATIO OF THE HEIGHT TO THE BASE; DIAMETER, OR RATIO OF AXES, of 4.00)

CYLINDER -	HORIZONTAL	1.32
	VERTICAL	1.07
PARALLELEPIPED WITH SQUARE BASE		
	HORIZONTAL	1.31
	VERTICAL	1.07
ELLIPSOIDS OF ROTATION		
	HORIZONTAL	1.28
	VERTICLE	1.36
TWO CIRCILAR CONES JOINED AT THEIR BASES		
	HORIZONTAL	1.27

GLASS SPHERES JOINED IN A CHAIN		
	TWO SPHERES	1.16
	THREE SPHERES	1.31
	FOUR SPHERES	1.70
	EIGHT SPHERES	2.14
	THREE FLAT DISKS	1.26
	SEVEN FLAT DISKS	1.70
	SIX OCTAHEDRA	1.31
SPECIFIC BODIES		
	OCTAHEDRON	1.06
	CUBE	1.07
	TETRAHEDRON	1.18

With the exception of a few of the large chain particles it appears that the variations in effective diameter is less than 20%. Thus, use of the basic sphere drag information with slight corrections for particle shape should give accurate results. Because of the wide variety in particle shapes and orientations it is impossible to suggest a specific statistical average for the shape factor. For spacelab applications the main interest will be in moving the aerosol particles to the filter system. Thus, for conservative calculations the drag coefficient should be selected somewhat smaller than expected.

The discussion of drag of aerosol has been limited to the case of rigid particles. If the particle is liquid it may deform or develope a circulation which alters the resistance to movement through the air. For a spherical drop with circulation the Stokes drag, eq. (17) is reduced by a factor, ref. 18

$$\frac{1 + (2\mu/3\mu_p)}{(1 + \mu/\mu_p)} \qquad (26)$$

where μ is the air viscosity and μ_p is the liquid droplet viscosity. For water in air the correction given by equation (26) is less than 1 percent. The liquid must be of low density for the circulation correction to be of importance.

Very large liquid droplets can be expected to breakup into smaller droplets that are stable. Obviously the stable droplet size is determined by the surface tension of the particular liquid.

CONCLUDING REMARKS

The major problem associated with dust in the Spacelab zero-gravity environment will be the failure of large particles to settle out of the air. Also the existance of g-jitter of the laborator will act to further keep the larger particles in suspension. Thus, it is necessary to examine the particle dynamics in the Reynolds number range from $1<R_e<100$. An exmaination of the measured data in this Reynolds number range led to the development of an emprical curve fit for the drag coefficient, c_D, of the form

$$c_D = \frac{24}{R_e}\left[1 + \frac{R_e^{0.7}}{6.8}\right]$$

A survey of experimental measurements of the drag of spheres over a wide range of flow conditions was evaluated. A graphic correlation of the drag coefficient as a function of both Reynolds and Knudsen number was developed. It was possible to cover a range of Knudsen number from zero to approximately 50. The present analysis was limited to a Reynolds number range between 10^{-2} and 10^{2}. Although information was lacking on the correlation of drag coefficient with Mach number at subsonic conditions, it was possible to include the limiting case of large supersonic Mach numbers.

The general equations governing the dust dynamics were reviewed.

REFERENCES

1. Boothroyd, R. G.; Flowing Gas-Solid Suspensions, Chapman and Hall Ltd., London, 1971.
2. Fuchs, N. A.; The Mechanics of Aerosols, MacMillan Co., N.Y., 1964.
3. Hidy, G. M., and Brock, J. R.; The Dynamics of Aerocolloidal Systems, Pergamon Press, 1970.
4. Soo, S. L.; Flight Dynamics of Multiphase Systems, Blaisdell. (Ginn), 1967.
5. Friedlander, S. K.; Smoke, Dust and Haze. John Wiley & Sons, N.Y., 1977.
6. Lumley, J. L.; Some Problems Connected with the Motion of Small Particles in Turbulent Motion. Ph.D. Thesis, John Hopkins Univ. 1957.
7. Cadle, R.D.; Particle Size, Reinhold Publishing Corp. N.Y., 1965.
8. Oseen, C., Ueber die Stokes'sche Formel, und uber eine verwandte Aufgabe in der Hydrodynamik, Arkiv for Matematik, Bd. vi. no 29 (1910).
9. Klyuchko, L.; Otopl. i ventil. no. 4, (1934).
10. Millikan, R.; Physics Review, vol. 22, p. 1, (1923).
11. Davies, C. N.; Proc. Phys. Soc, Vol. 57, p. 259, (1945).
12. Phillips, W. M., and Kuhlthau, A. R.; Drag Measurements on Magnetically Supported Spheres in Low Density High Speed Flow. Adv. in Applied Mech. Supplement 5, vol. 1, Rarefied Gas Dynamics, p. 711, (1969).
13. Sims, W. H.; Experimental Sphere Drag Results in the Near-Free Molecule Regine. Adv. in Applied Mech. Supplement 5, vol. 1, Rarefied Gas Dynamics, p. 751, (1969).
14. Kavanau, L. L.; Heat Transfer from Spheres to a Rarefied Gas in Subsonic Flow. Trans. ASME, vol. 77, p. 617, (1955).
15. Baldwin, L. V., Sandborn, V. A., and Laurence, J. C.; Heat Transfer from Transverse and Yawed Cylinders in Continuum, Slip and Free Molecule Flow. Jour. of Heat Transfer, Trans. ASME, vol. 82, series C, no. 2, p. 77, (1960).
16. Schaaf, S. A. and Chambre, P. L.; Flow of Rarefied Gases. High Speed Aerodynamics and Jet Propulsion. vol. III, section H (edited by H. W. Emmons). Princeton University Press, (1958).

17. Perrin, F.; Jour. Physs. Radium, ser. 7, vol. 7, p. 1, (1936).
18. Rybczinski, W. Anzeig. Akad. Krakau, vol. 40, (1911).

1. REPORT NO.	2. GOVERNMENT ACCESSION NO.	3. RECIPIENT'S CATALOG NO.
NASA CR-3158		

4. TITLE AND SUBTITLE	5. REPORT DATE
Particle Dynamics Associated with the Spacelab Environment	July 1979
	6. PERFORMING ORGANIZATION CODE

7. AUTHOR(S)	8. PERFORMING ORGANIZATION REPORT #
V. A. Sandborn	Research Memorandum 38

9. PERFORMING ORGANIZATION NAME AND ADDRESS	10. WORK UNIT NO.
College of Engineering Colorado State University Fort Collins, Colorado 80521	M-285
	11. CONTRACT OR GRANT NO.
	NAS8-31688
	13. TYPE OF REPORT & PERIOD COVERED
12. SPONSORING AGENCY NAME AND ADDRESS	Contractor
National Aeronautics and Space Administration Washington, D. C. 20546	14. SPONSORING AGENCY CODE

15. SUPPLEMENTARY NOTES

Prepared under the technical monitorship of the Atmospheric Sciences Division, Space Sciences Laboratory, NASA Marshall Space Flight Center

16. ABSTRACT

The problem of dust in the microgravity environment of Spacelab is reviewed. A major factor in dust dynamics in a microgravity environment is the absence of settling; hence Spacelab air will contain larger particles than a comparable laboratory on Earth. In addition, the presence of low-level acceleration fluctuations (thruster firings, crew motions, etc.) could inhibit dust removal by surface scavenging. Because of the presence of larger particles, aerosol dynamics at larger Reynolds numbers must be considered. An accurate drag coefficient for spherical particles is developed for the higher Reynolds number phenomena. A general graphic correlation for the drag coefficient as a function of Reynolds and Knudsen numbers was developed based on currently available drag data for spheres. The general equations that govern dust dynamics are reviewed.

17. KEY WORDS	18. DISTRIBUTION STATEMENT
Particle dynamics Microgravity environment	Category 34

19. SECURITY CLASSIF. (of this report)	20. SECURITY CLASSIF. (of this page)	21. NO. OF PAGES	22. PRICE
Unclassified	Unclassified	28	$4.00

* For sale by the National Technical Information Service, Springfield, Virginia 22161

NASA-Langley, 1979